Exact solution of Maxwell's equations for optical interactions with a macroscopic random medium

Snow H. Tseng, Jethro H. Greene, and Allen Taflove

Department of Electrical and Computer Engineering, Northwestern University, Evanston, Illinois 60208

Duncan Maitland

Medical Physics and Biophysics Division, Lawrence Livermore National Laboratory, Livermore, California 94550

Vadim Backman and Joseph T. Walsh, Jr.

Department of Biomedical Engineering, Northwestern University, Evanston, Illinois 60208

Received December 11, 2003

We report what we believe to be the first rigorous numerical solution of the two-dimensional Maxwell equations for optical propagation within, and scattering by, a random medium of macroscopic dimensions. Our solution is based on the pseudospectral time-domain technique, which provides essentially exact results for electromagnetic field spatial modes sampled at the Nyquist rate or better. The results point toward the emerging feasibility of direct, exact Maxwell equations modeling of light propagation through many millimeters of biological tissues. More generally, our results have a wider implication: Namely, the study of electromagnetic wave propagation within random media is moving toward exact rather than approximate solutions of Maxwell's equations. © 2004 Optical Society of America

OCIS codes: 240.6680, 060.0060, 060.2320, 240.6690, 170.3880, 290.7090.

Tissue optics deals with light scattering by biological structures, on which noninvasive optical imaging techniques such as optical coherence tomography are based. Most studies of tissue optics have utilized heuristic approximations in the categories of radiative transfer theory[1] and Mie theory,[2] including Beer's law, the Kubelka–Monk theory, the adding–doubling method, the diffusion approximation, and the Monte Carlo method. To various degrees, these methods neglect the full-vector electromagnetic wave nature of light based on Maxwell's equations, especially with regard to near-field interactions of closely spaced particles.

Recently, finite-difference time-domain numerical solutions of Maxwell's equations[3] were applied to model optical interactions with models of single biological cells.[4] In principle, the finite-difference time-domain method (FDTD) could be used to model cell collections spanning macroscopic dimensions (millimeters) and thus to attack the tissue-optics problem on the most fundamental basis. However, using the FDTD may not be feasible for many years because computers lack capabilities to deal with the enormous database of electromagnetic field vector components mandated for the FDTD by its mesh-density requirement of 20 or more samples per optical wavelength in each spatial dimension.

In this Letter we report the initial application to the tissue-optics problem of an emerging advanced variant of the FDTD: the pseudospectral time-domain technique (PSTD).[5,6] For large electromagnetic wave interaction models in D dimensions that do not have geometric details or material inhomogeneities smaller than one-half wavelength the PSTD reduces computer storage and running time by approximately 8^D:1 relative to standard the FDTD while it achieves comparable accuracy.[5,6] This advantage is sufficient to permit, for the first time to the authors' knowledge rigorous numerical solution of the full-vector Maxwell equations for optical propagation within, and scattering by, a random medium of macroscopic dimensions.

The most basic version of the PSTD is implemented on an unstaggered, collocated Cartesian space grid. Let $\{V_i\}$ denote the values of field component V at all points along an x-directed cut through the grid, and let $\{(\partial V/\partial x)_i\}$ denote the x derivatives of V at the same points needed in Maxwell's equations. Using the differentiation theorem for Fourier transforms, we can write

$$\left\{\frac{\partial V}{\partial x}\,\middle|_i\right\} = -\mathbf{F}^{-1}(j\tilde{k}_x\mathbf{F}\{V_i\}), \tag{1}$$

where $\mathbf{F}$ and $\mathbf{F}^{-1}$ denote, respectively, the forward and inverse discrete Fourier transform and $\tilde{k}_x$ is the Fourier transform variable that represents the x component of the numerical wave vector. In this way, $\{(\partial V/\partial x)_i\}$ can be calculated in one step. In multiple dimensions, this process is repeated for each cut parallel to one of the major axes of the space lattice.

According to the Nyquist sampling theorem, the representation in Eq. (1) is exact (i.e., of infinite order) for electromagnetic field spatial modes sampled at the Nyquist rate or better. This permits the PSTD's meshing density to approach two samples per wavelength in each spatial dimension. The wraparound caused by the periodicity in the discrete Fourier transform is eliminated by use of the anisotropic perfectly matched layer absorbing boundary condition.[7]

We introduce an arbitrary incident wave by implementing the scattered-field formulation.[3] Here,

0146-9592/04/121393-03$15.00/0

the total electric (E) and magnetic (H) fields within the grid are decomposed into a sum of unknown scattered fields ($\mathbf{E}_{\text{scat}}, \mathbf{H}_{\text{scat}}$) and known incident fields ($\mathbf{E}_{\text{inc}}, \mathbf{H}_{\text{inc}}$) propagating in a lossless vacuum. Following Ref. 3, we write Maxwell's curl equations for this case as

$$\mu \frac{\partial \mathbf{H}_{\text{scat}}}{\partial t} + \sigma^* \mathbf{H}_{\text{scat}} = -\nabla \times \mathbf{E}_{\text{scat}} - \sigma^* \mathbf{H}_{\text{inc}} - (\mu - \mu_0) \frac{\partial \mathbf{H}_{\text{inc}}}{\partial t}, \quad (2)$$

$$\epsilon \frac{\partial \mathbf{E}_{\text{scat}}}{\partial t} + \sigma \mathbf{E}_{\text{scat}} = \nabla \times \mathbf{H}_{\text{scat}} - \sigma \mathbf{E}_{\text{inc}} - (\epsilon - \epsilon_0) \frac{\partial \mathbf{E}_{\text{inc}}}{\partial t} \quad (3)$$

in a source-free region where material parameters μ, ϵ, σ^*, and σ are mapped into the grid to specify the geometry. Space derivatives of ($\mathbf{E}_{\text{scat}}$, $\mathbf{H}_{\text{scat}}$) are implemented by means of Eq. (1), and time stepping is implemented by the Yee leapfrog.[3,5,6] The total E and H fields are obtained in a postprocessing step by addition of the PSTD-computed scattered fields to the known incident fields.

The PSTD has been extensively validated.[5,6,8] For electromagnetic wave interaction structures whose primary geometrical or material feature sizes exceed one half of the dielectric wavelength (λ_d), the PSTD has been shown to exhibit the same computational accuracy and dynamic range as FDTDs that have approximately eight-times-finer resolution.[5,6] That is, a PSTD grid with coarse $\lambda_d/4$ resolution provides approximately the same accuracy as a FDTD grid with fine $\lambda_d/32$ resolution. Much experience with FDTD modeling has shown that this level of spatial resolution yields an accuracy of better than 1 dB over dynamic ranges that exceed 50 dB for the scattering intensity observed at all possible angles, including backscatter.[3] For the millimeter-scale optical paths of great current interest in biophotonics, we expect PSTD grids with $\lambda_d/4$ resolution to provide comparable accuracy and dynamic range.

In this Letter we report the initial application of the PSTD to model two-dimensional transverse-magnetic scattering of light by large bundles of infinitely long dielectric cylinders in free space. We use a PSTD grid that has a uniform spatial resolution of 0.25 μm, equivalent to $0.3\lambda_d$ at 300 THz for cylinder refractive index $n = 1.2$. Figure 1 shows the PSTD-computed total scattering cross section (TSCS) of a 160-μm overall-diameter cylindrical bundle of 34 randomly positioned, noncontacting, dielectric cylinders of diameter d. For each of the cases studied ($d = 5$, 10, 15, 20 μm), a single PSTD run provides a frequency response of 0.5–300 THz ($\lambda_0 = 60$–1 μm) with a resolution of 0.5 THz. Note that the position of the center of each cylinder is fixed for each case. We can see that, as d exceeds approximately 10 μm, the bundle's TSCS above 60 THz saturates.

Figure 2 shows the PSTD-computed TSCS of a 160-μm overall-diameter cylindrical bundle of N randomly positioned, noncontacting $n = 1.2$ dielectric cylinders of individual diameter $d = 5$ μm. Here, five cases are shown ($N = 80$, 200, 320, 400, 480). We see that, as N exceeds approximately 200, the TSCS above 60 THz saturates at the level indicated in Fig. 1.

Figure 3 shows results analogous to those of Fig. 2 for a bundle of N dielectric cylinders for individual diameter $d = 10$ μm. Five cases are shown ($N = 20$, 50, 80, 100, 120). As N exceeds approximately 50, the TSCS above 60 THz saturates at the same level as in Figs. 1 and 2.

Together, Figs. 1–3 show that a saturation effect for the TSCS of a fixed-overall-sized bundle of randomly positioned, noncontacting cylinders can be achieved in different ways. In Fig. 1 the position and number of the cylinders within the bundle are constant, while the diameter of each cylinder increases. In Figs. 2 and 3 the diameter of each cylinder is constant, while the total number of cylinders within the bundle increases. As the average dielectric coverage of each bundle increases beyond a certain threshold, the TSCS of the bundle becomes independent of its internal geometric details such as the size, position, and number of its constituent cylinders.

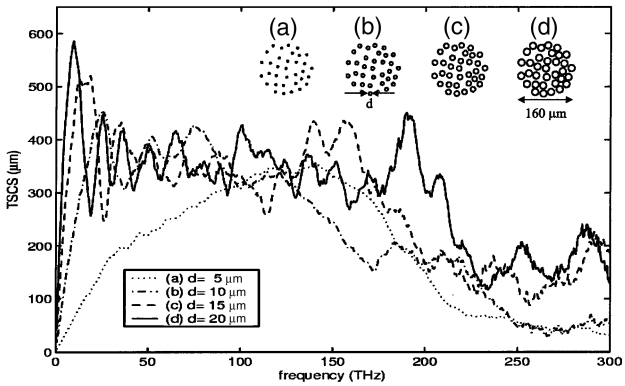

Fig. 1. PSTD-computed TSCS of a 160-μm overall-diameter cylindrical bundle of 34 randomly positioned, noncontacting $n = 1.2$ dielectric cylinders of individual diameter d. Four cases [(a)–(c)] are shown, with the position of each cylinder fixed. As d exceeds approximately 10 μm, the TSCS above 60 THz saturates.

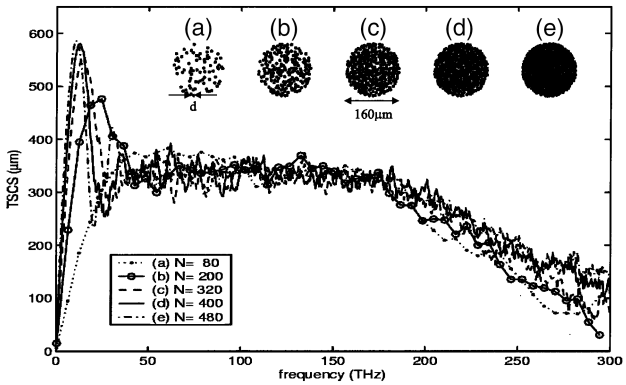

Fig. 2. PSTD-computed TSCS of a 160-μm overall-diameter cylindrical bundle of N randomly positioned, noncontacting $n = 1.2$ dielectric cylinders of fixed individual diameter $d = 5$ μm. Five cases [(a)–(e)] are shown. As N exceeds approximately 200, the TSCS above 60 THz saturates at the level indicated in Fig. 1.

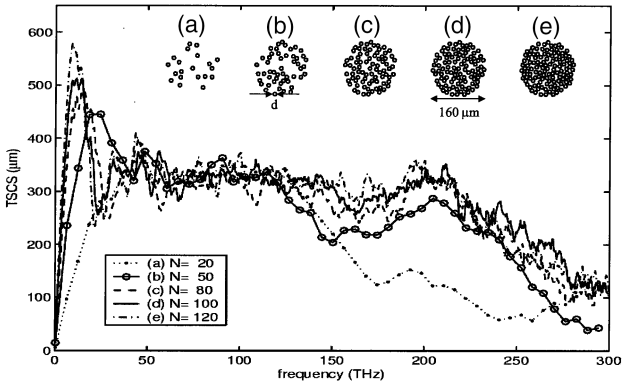

Fig. 3. PSTD-computed TSCS of a 160-μm overall-diameter cylindrical bundle of N randomly positioned, noncontacting $n = 1.2$ dielectric cylinders of fixed individual diameter $d = 10$ μm. Five cases [(a)–(e)] are shown. As N exceeds approximately 50, the TSCS above 60 THz saturates at the same level as in Figs. 1 and 2.

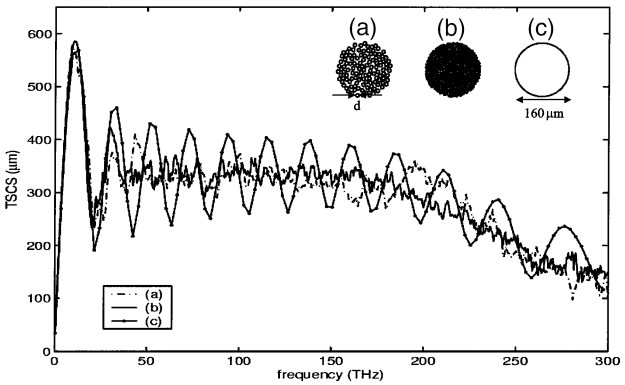

Fig. 4. PSTD-computed TSCSs of (a) a 160-μm overall-diameter cylindrical bundle of 120 randomly positioned, noncontacting $n = 1.2$ dielectric cylinders of individual diameter $d = 10$ μm; (b) as in (a) but for 480 cylinders of individual diameter $d = 5$ μm; (c) a single cylinder of refractive index $n = 1.0938$, the average refractive index for (a) and (b).

This conclusion is further supported by Fig. 4, which illustrates the PSTD-computed TSCSs of (a) a 160-μm overall-diameter cylindrical bundle of 120 randomly positioned, noncontacting $n = 1.2$ dielectric cylinders of individual diameter $d = 10$ μm; (b) as in (a) but for 480 cylinders of individual diameter 5 μm; and (c) a single cylinder of refractive index $n = 1.0938$, the volume-averaged refractive index in (a) and (b). We can see that the frequency dependence of the TSCSs of the bundles of (a) and (b) represents essentially the average behavior of the TSCS of the volume-averaged homogeneous cylinder of (c). The primary difference is that the homogeneous cylinder exhibits ripples of its TSCS versus frequency as a result of coherent internal wave-interference effects that are suppressed by scattering events within the random clusters.

We have reported what we believe to be the first rigorous numerical solution of the two-dimensional Maxwell equations for optical propagation within, and scattering by, a random medium of macroscopic dimensions. Our solution is based on the pseudo-spectral time-domain technique, which provides essentially exact results for electromagnetic field spatial modes sampled at the Nyquist rate or better. In ongoing research we have found that it is straightforward to extend the PSTD to the full-vector Maxwell equations in three dimensions. We have validated PSTD models of scattering by isolated spheres and are commencing studies of optical interactions with millimeter-scale three-dimensional volumes of biological tissues.

The results reported in this Letter point toward the emerging feasibility of direct, exact Maxwell-equations modeling of light propagation through, and scattering by, millimeters of biological tissues. More generally, our results have a wider implication. Namely, the study of electromagnetic wave propagation within random media is moving toward exact rather than approximate solutions of Maxwell's equations.

The authors thank Zhigang Chen for helpful technical discussions. Also, the authors thank the National Institutes of Health National Cancer Institute (contract grant 5R01CA085991-03) and the Pittsburgh Supercomputing Center (grant ECS020006P) for their support of this research. This study was performed under the auspices of the U.S. Department of Energy under contract W-7405-ENG-48. S. H. Tseng's e-mail address is snow@ece.northwestern.edu.

References

1. A. J. Welch and M. J. C. van Gemert, in *Lasers, Photonics, and Electro-Optics*, H. Kogelnik, ed. (Plenum, New York, 1995).
2. G. Mie, Ann. Phys. (Leipzig) **25,** 377 (1908).
3. A. Taflove and S. C. Hagness, *Computational Electrodynamics: the Finite-Difference Time-Domain Method* (Artech House, Boston, Mass., 2000).
4. R. Drezek, A. Dunn, and R. Richards-Kortum, Opt. Express **6,** 147 (2000), http://www.opticsexpress.org.
5. Q. H. Liu, Microwave Opt. Technol. Lett. **15,** 158 (1997).
6. Q. H. Liu, IEEE Trans. Geosci. Remote Sens. **37,** 917 (1999).
7. S. D. Gedney, IEEE Trans. Antennas Propag. **44,** 1630 (1996).
8. G. Zhao and Q. H. Liu, IEEE Trans. Antennas Propag. **51,** 619 (2003).